Self-Induced Preparation of Assembled Shrubbery TiSi Nanowires by Chemical Vapor Deposition

ARTICLE *in* CRYSTAL GROWTH & DESIGN · SEPTEMBER 2008

Impact Factor: 4.89 · DOI: 10.1021/cg7008545

10 AUTHORS, INCLUDING:

Jun Du
Nanchang University
16 PUBLICATIONS **71** CITATIONS
SEE PROFILE

Piyi Du
Zhejiang University
264 PUBLICATIONS **2,250** CITATIONS
SEE PROFILE

CRYSTAL GROWTH & DESIGN
2008
VOL. 8, NO. 10
3543–3548

Self-Induced Preparation of Assembled Shrubbery TiSi Nanowires by Chemical Vapor Deposition

Jun Du,[†,‡] Zhaodi Ren,[†] Kaiying Tao,[†] Anhong Hu,[†] Peng Hao,[†] Yanfei Huang,[†] Gaoling Zhao,[†] Wenjian Weng,[†] Gaorong Han,[†] and Piyi Du*[,†]

State Key Laboratory of Silicon Materials, Department of Materials Science and Engineering, Zhejiang University, Hangzhou 310027, China, and Department of Chemical Engineering, Nanchang University, Nanchang 330029, China

Received September 7, 2007; Revised Manuscript Received June 20, 2008

ABSTRACT: We report a new self-induced catalyst-free method for the preparation of shrubbery TiSi nanowires by atmospheric pressure chemical vapor deposition. SiH_4 and $TiCl_4$ are used as a silicon precursor and titanium precursor, respectively. Ti_5Si_3 thin films are formed initially, and then one-dimensional TiSi nanostructures are grown on top of the thin films. A novel, assembled structure with electrically conductive shrubbery TiSi nanowires with an electrically conductive Ti_5Si_3 thin layer underneath is finally obtained. The TiSi nanowires grow along the direction perpendicular to the (110) plane of the orthorhombic TiSi crystal. The nanowires are more than 5 μm long, and their diameters are about 15−40 nm. With the flux of (SiH_4 + $TiCl_4$) reaching values larger than 35 sccm or increasing from 20 to 35 sccm, the quantities of TiSi nuclei are increased and, thus, the TiSi nanowire bundles and rocket-shaped nanowires are also successfully prepared, respectively. With regard to producing a high storage capacitor with the nanowire bottom electrode embedded within the dielectric thin film of $Ba_{0.6}Sr_{0.4}TiO_3$ (BST), the capacitance of the BST/assembled-nanowire-electrode complex structure is about 28 pF, which is approximately 3 times higher than that of BST deposited on indium-tin oxide (ITO). This creates a new way to fabricate the thin film devices with a high storage capacitance.

1. Introduction

Finding a new way to grow nanowires is important, as it would provide a significant breakthrough in broad applications of nanowires.[1] The growth of nanowires induced by as-deposited homogeneous substances, rather than other metal catalysts,[2−4] is a good way to prepare high purity nanowires. If the high purity, electrically conductive nanowires can grow on the electrically conductive thin film, not only will the electrode area increase enormously, but the fringing electric fields radiated from the nanowires can also be used effectively.[5] This method would blaze a new trail in the fabrication and development of a thin film device with a high storage capacitance.[6−9]

Metal silicides, which have been widely used in ultra large scale integration technologies,[10] are excellent candidates for nanowire electrodes due to their high conductivity and thermal stability. At present, one-dimensional nanostructures of metal silicides, such as $CoSi_2$,[11] $ErSi_2$,[12] NiSi,[13] Pt_6Si_5,[14] $TiSi_2$,[15] and some rare-earth silicides,[16] have been successfully prepared by the solid reaction method. Furthermore, applications of the nanowires are being sought. For the titanium silicide nanowires formed on Si, an efficient, homogeneous, and stable field emission was observed, indicating a potential application in vacuum microelectronics, especially in flat panel displays.[15] Since atmospheric pressure chemical vapor deposition (APCVD) is an economical process for continuous and large-scale production and probably can be used for depositing on required substrates,[17] it is important to find an APCVD method to grow silicide nanowires for future uses, such as for glass-based large-scale field emission devices and, especially, for thin film capacitors.

In this paper, we report a new, controllable method for the preparation of shrubbery TiSi nanowires by APCVD. A novel assembled structure incorporating electrically conductive shrubbery TiSi nanowires and electrically conductive thin Ti_5Si_3 layer underneath is obtained, and the dielectric properties of the assembled structure are investigated.

2. Experimental Section

2.1. Preparation. Ti_5Si_3 thin films and TiSi nanowires were both prepared on borosilicate glass substrates in a hot-wall quartz reactor. SiH_4 and $TiCl_4$ were used as a silicon precursor and titanium precursor, respectively. Nitrogen was used as the carrier gas, which flowed through two bubblers carrying $TiCl_4$ to the reaction chamber.[18] Ti_5Si_3 thin films were formed initially, and then one-dimensional TiSi nanostructures were grown on top of it. The deposition temperature ranged from 690 to 700 °C. The total gas flux (including the N_2) was 1000 sccm. For Ti_5Si_3 thin films, the molar ratio of $SiH_4/TiCl_4$ was 1, and the flux of (SiH_4 + $TiCl_4$) was 24 sccm for 2 min. For nanowires, the molar ratio of $SiH_4/TiCl_4$ was 1.5, and the flux of the source gases (not including N_2) was 20 sccm for 15 min. For TiSi nanowires bundles, the molar ratio of $SiH_4/TiCl_4$ was 1.5, and the flux of (SiH_4 + $TiCl_4$) was 35 sccm. For rocket-shaped nanowires, the molar ratio of $SiH_4/TiCl_4$ was 1.5, and the flux of the source gas was initially kept at 20 sccm for 10 min and then increased to a higher flux for 5 min. N_2 was introduced into the reaction chamber when the temperature was decreased from the deposition temperature to room temperature. To prepare a TEM specimen, sample pieces were scraped from the glass substrate, suspended in ethanol, and dropped on a carbon copper grid.

$Ba_{0.6}Sr_{0.4}TiO_3$ (BST), which is an important ferroelectric oxide that is widely used in electronic devices because of its high dielectric constant and low leakage current,[19] was prepared on the assembled nanowire structure and ITO glass by a sol−gel process with a dip coating method. The samples were dried at 200 °C for 20 min after the BST thin films were dip coated on the substrates. Then, the two samples were annealed in air at 600 °C for 1 h. The top gold electrode used to measure the capacitance of the BST was deposited by covering the mask with an aperture of 0.1 mm on the surface of the thin film.

2.2. Characterization. A field emission scanning electron microscope (FESEM, SIRON, FEI) was used to identify the morphology of the as-deposited material. X-ray diffractometry (XRD) was performed to characterize the phase structure of the samples. Transmission electron microscope (TEM) and high-resolution TEM (HRTEM) images were

* To whom correspondence should be addressed. E-mail: dupy@zju.edu.cn. Tel: +86-571-87952324. Fax: +86-571-87952341.
† Zhejiang University.
‡ Nanchang University.

10.1021/cg7008545 CCC: $40.75
Published on Web 09/05/2008

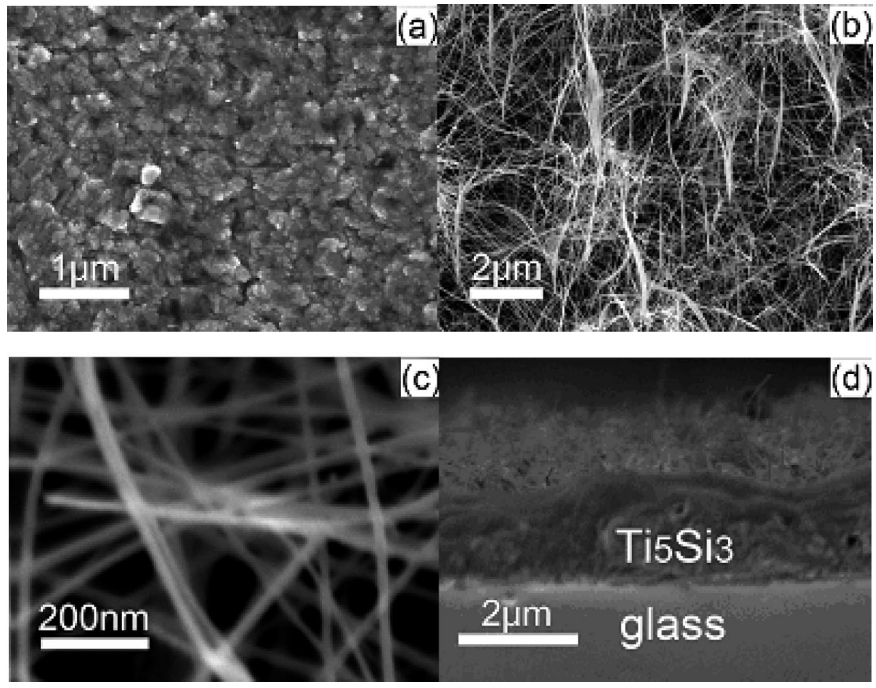

Figure 1. SEM image of (a) Ti_5Si_3 thin films on the glass, (b) shrubbery TiSi nanowires, (c) enhanced shrubbery TiSi nanowires and (d) cross-section of assembled structure.

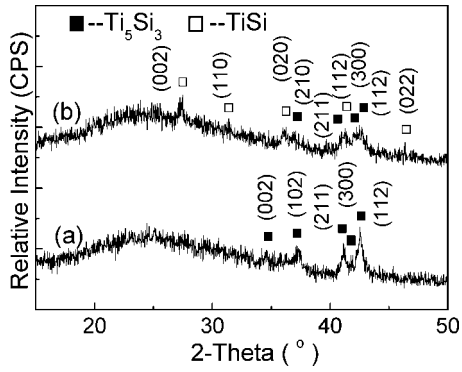

Figure 2. XRD patterns of (a) Ti_5Si_3 thin films on glass and (b) TiSi nanowires on Ti_5Si_3 thin films, respectively, prepared by APCVD.

obtained on a JEOL-2010 HRTEM using an acceleration voltage of 200 kV. An Agilent 4294A precision impedance analyzer was employed to measure the dielectric properties of the samples.

3. Results and Discussion

Figure 1a shows the FESEM micrograph of Ti_5Si_3 thin films deposited on glass substrates. The size of the particles is about 300 nm. Figure 1b,c shows TiSi nanowires formed on Ti_5Si_3 thin films. The length of the nanowires is more than 5 μm, and their diameters are about 15−40 nm. Figure 1d shows the cross sectional figure of the layered configuration, as well as exhibiting the TiSi shrubbery nanowires grown on the titanium silicide bottom layer which formed on the glass substrate. The XRD patterns of the Ti_5Si_3 thin film and TiSi nanowires are shown in Figure 2. The diffraction peaks in Figure 2a can be readily indexed to a hexagonal structure with cell constants of $a = 0.743$ and $c = 0.517$ nm, demonstrating that the thin film is Ti_5Si_3. The XRD pattern shown in Figure 2b demonstrates that orthorhombic TiSi nanowires are formed. The lattice constants of TiSi are $a = 0.3610$ nm, $b = 0.4965$ nm and $c = 0.6500$ nm. A TEM image of one of these nanowires is shown in Figure 3a. It shows that the diameter is about 35 nm, in good agreement with the FESEM data. The HRTEM image of the nanowires is shown in Figure 3b. The lattice spacings of the nanowire, which are 0.32, 0.29, and 0.22 nm, are consistent with the *d*-spacings of the (002), (110), and (112) crystallographic planes of TiSi. Thus, the nanowire is confirmed to be a single crystal phase of TiSi. The growth direction of the TiSi nanowires is obviously along the direction perpendicular to its (110) plane.

The assembled structure of the shrubbery TiSi nanowires growing on the Ti_5Si_3 thin layer shows that the nanowire can grow on the surface of the homogeneous base layer as-deposited. It may be related to the formations of TiSi and Ti_5Si_3 during deposition. It is obvious that Ti_5Si_3 forms when the molar ratio of $SiH_4/TiCl_4$ is 1. The main reaction is

$$5TiCl_4(g) + 5SiH_4(g) = Ti5Si_3(s) + 2SiCl_4(g) + 12HCl(g) + 4H_2(g) \quad (1)$$

After the molar ratio of $SiH_4/TiCl_4$ increases from 1 to 1.5, the main reaction is

$$2TiCl_4(g) + 3SiH_4(g) = 2TiSi(s) + SiCl_4(g) + 4HCl(g) + 4H_2(g) \quad (2)$$

The Gibbs free energies[20] of the two reactions at a temperature of about 700 °C are $\Delta rG_1 = -256.998$ kJ/mol and $\Delta rG_2 = -274.060$ kJ/mol, respectively. According to the Gibbs free energy of the reactions, the reaction forming TiSi becomes important as the molar ratio of $SiH_4/TiCl_4$ increases to 1.5, as shown in eq 2. In fact, TiSi can form in a one-dimensional nanostructure on the Ti_5Si_3 base-layer in this case. It is likely that a vapor-solid growth process[21] dominates the growth of the TiSi nanowires. After the active dot of TiSi is formed on the homogeneous base, continuous feeding of Ti and Si into the TiSi nanoparticles can lead to 1D growth of the TiSi crystalline phase.

In addition to the normal nanowires, other nanostructures have also been formed under different growth conditions. Figure 4

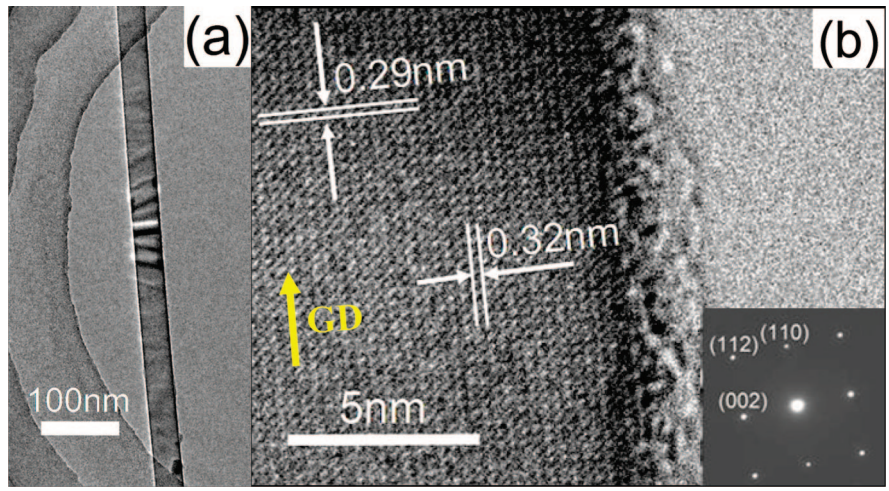

Figure 3. Characterization of TiSi nanowires. (a) TEM image, (b) HRTEM image of a TiSi nanowire. The inset is its electron diffraction pattern. Abbreviation GD denotes growth direction.

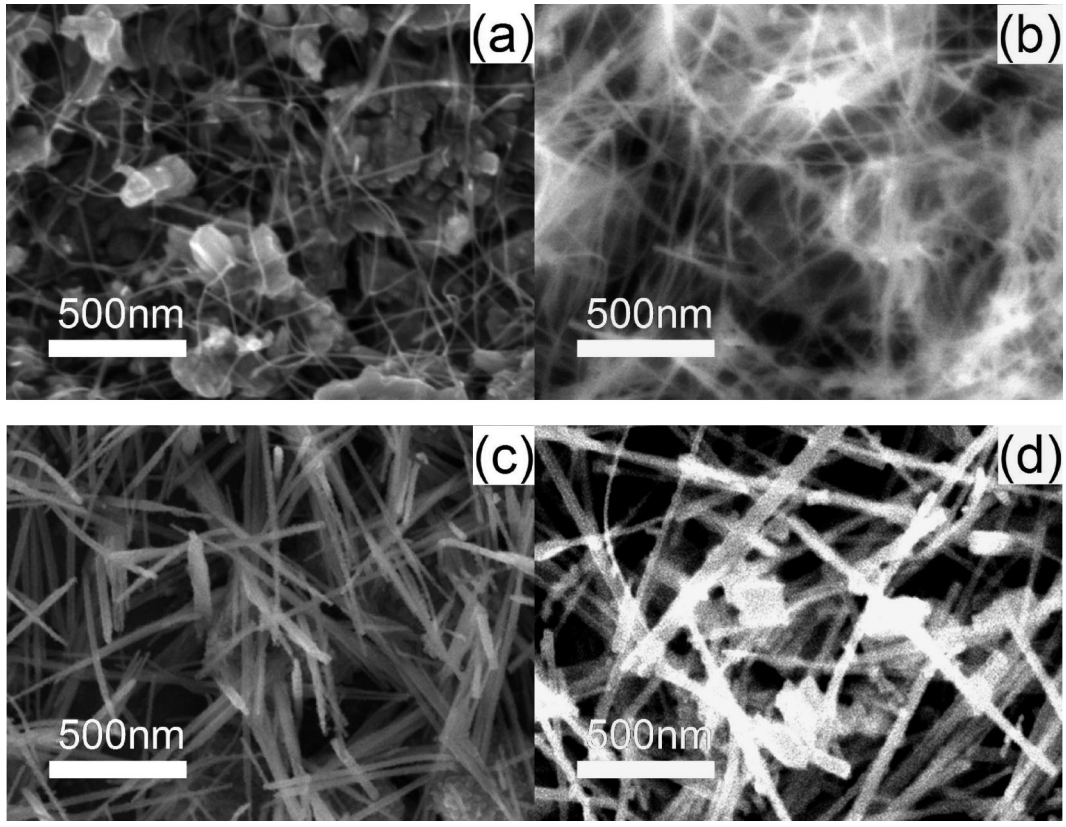

Figure 4. FESEM micrographs of TiSi nanowire bundles prepared on glass at 690 °C using a flux of (SiH_4 + $TiCl_4$) of (a) 15, (b) 17.5, (c) 25 and (d) 35 sccm.

shows the nanowires prepared under different fluxes of SiH_4 and $TiCl_4$ with a molar ratio of 3:2. With a lower flux of gas sources, as shown in Figure 4a,b, the thin flexible nanowires seem to form on the base layer. With an increase of the gas source flux, their diameter increases from 10 to 20 nm and the density of the nanowires increases greatly. However, with a higher flux of the gas sources, as shown in Figure 4c,d, thick hard nanowires seem to form. The density of the nanowires does not obviously increase, although the diameter of the nanowires increases from about 20 nm to 40−70 nm. Figure 5a shows the TEM image of the big nanowire from the sample, as shown in Figures 4d and 5b, as well as showing its electron diffraction pattern of the nanowire. To our surprise, the big nanowire consists of several parallel nanowires. It is actually a nanowire bundle. The nanowire bundle is also confirmed to be a single crystal phase of TiSi, as shown in Figure 5b.

In fact, the concentrations of (SiH_4 + $TiCl_4$) have an important influence on the quantities of TiSi nanowires. When the flux of (SiH_4 + $TiCl_4$) is low, the number of TiSi nuclei is low and, thus, the quantity of TiSi nanowires is small. With an increasing flux of (SiH_4 + $TiCl_4$) (from 15 to 25 sccm), the number of TiSi nuclei and, thus, the density of TiSi nanowires increases. As shown in Figure 4a, only a few thin nanowires form when the flux of (SiH_4 + $TiCl_4$) is 15 sccm. In contrast,

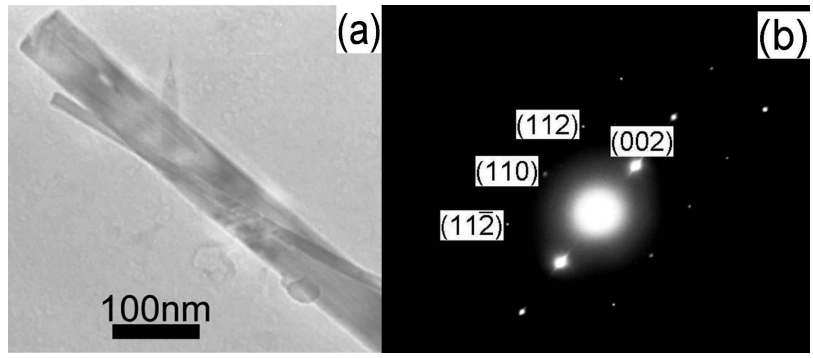

Figure 5. Characterization of TiSi nanowire bundle. (a) TEM micrograph and (b) electron diffraction pattern of a TiSi nanowire bundle.

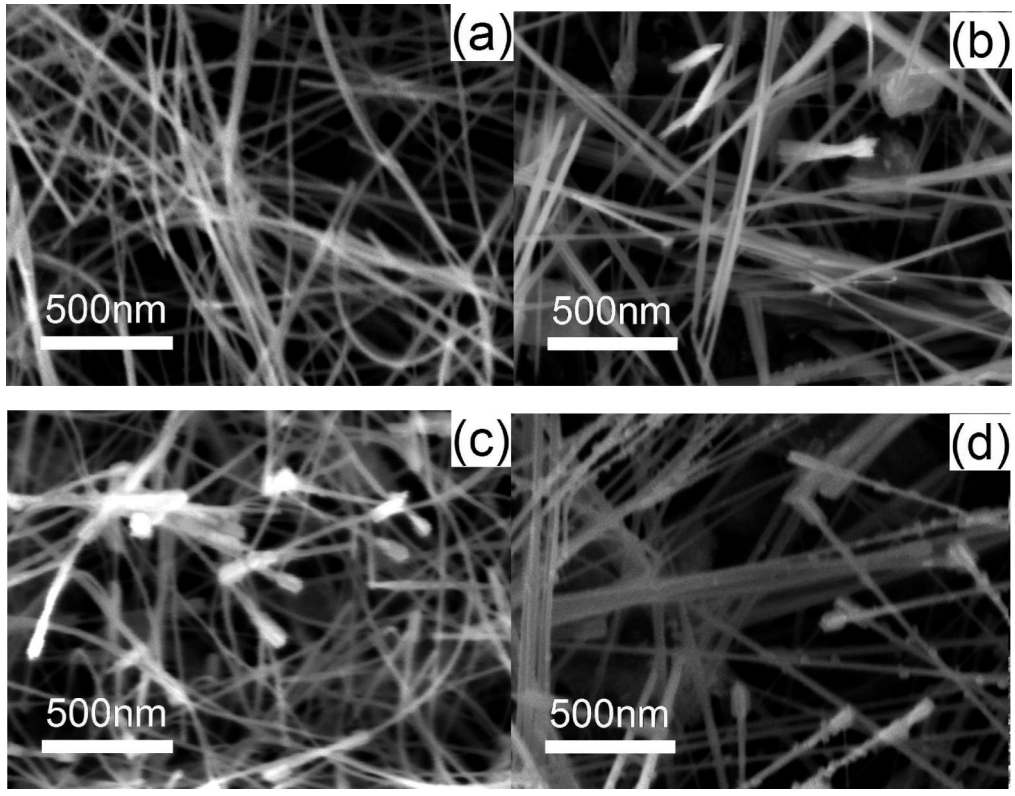

Figure 6. FESEM micrographs of TiSi rocket-shaped nanowires prepared on glass at 700 °C using a flux of (SiH_4 + $TiCl_4$) of (a) 20, (b) 25, (c) 35 and (d) 40 sccm for 5 min after a flux of (SiH_4 + $TiCl_4$) of 20 sccm for 10 min.

the nanowires are densely formed under a flux of (SiH_4 + $TiCl_4$) of 17.5 sccm (Figure 4b). With the flux of the source gases increasing to 25 and 35 sccm, the thick hard nanowire forms with increasing density, as compared to that in the case of low flux. In particular, when the flux is higher than 35 sccm, the neighboring nanowires contact each other due to increased numbers of TiSi nuclei. The nanowire bundles then form, as shown in Figure 4d.

In addition to the TiSi nanowire bundles that have been successfully prepared with the higher gas source flux of 35 sccm, a new shape of nanowire forms when the flux of source gases is increased from 20 sccm to a higher value (35 sccm) while the TiSi nanowires are forming. Figure 6 shows the FESEM images of these samples. A large tip forms on the nanowires. Their TEM images are shown in Figure 7. The nanowire tip consists of several parallel nanowires that encircle the long nanowire. It looks like a rocket-shaped nanowire. The electron diffraction pattern of the rocket-shaped nanowire, as shown in Figure 7c, is the same as the normal nanowires. It shows that the rocket-shaped nanowire is also a single crystal phase of TiSi.

The number of TiSi nuclei undoubtedly increases with the flux of the source gases. When the flux of the source gases is fixed as 20 sccm, as shown in Figure 6a, the normal nanowires form. When the flux of the source gases increases from 20 to 35 sccm, the formation of TiSi keeps increasing. Some increased TiSi will be deposited on the tip of the nanowires and form a new TiSi nucleus. Due to the induction effect of TiSi nanowires, these new nuclei will also form nanowires. Thus, several short parallel nanowires encircle the central long nanowire. In fact, when the TiSi island nucleation occurs on the growing nanowires, on the one hand, the original nanowires will give an inducement to the subsequent nanowires; on the other hand, the subsequent nanowires grown in the direction perpendicular to the (110) plane will lead to effective self-inducing growth due to the lowest surface free energy easily appearing outside the nanowire. Therefore, when grown parallel to the original

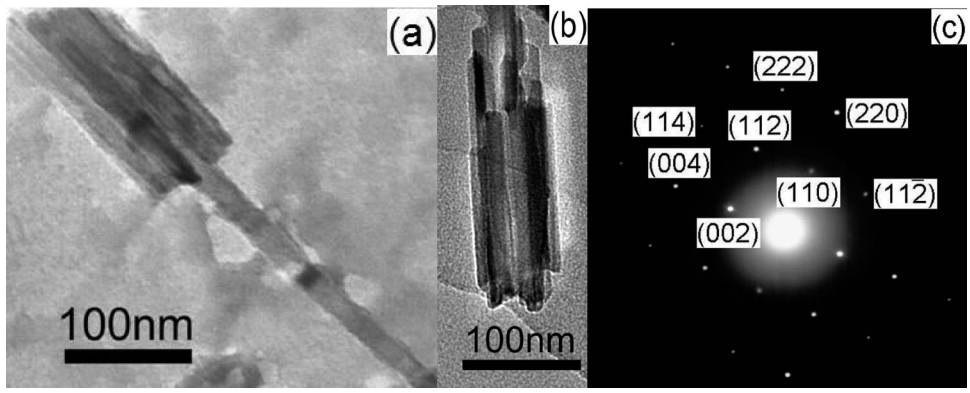

Figure 7. Characterization of TiSi rocket-shaped nanowires. (a) and (b) are the TEM micrographs of TiSi rocket-shaped nanowire. (c) Electron diffraction pattern of a TiSi rocket-shaped nanowire.

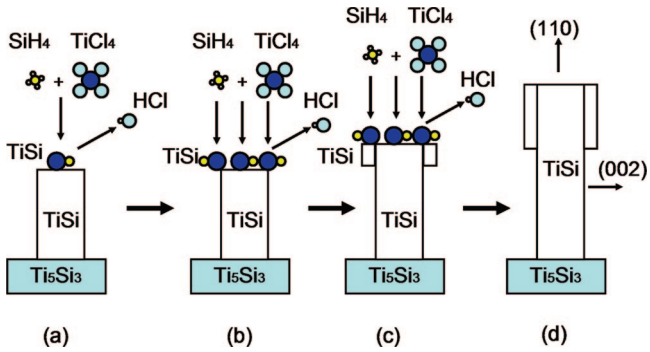

Figure 8. Schematic diagram of the formation of a rocket-shaped TiSi nanowire.

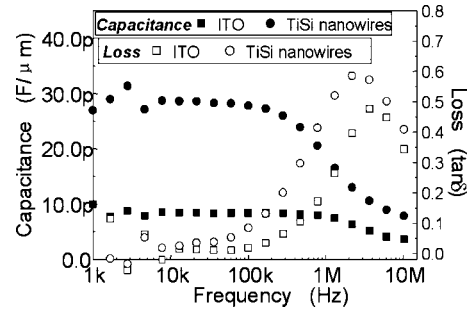

Figure 9. C-f and L-f curves of BST thin film with and without the nanowire-assembled bottom electrode.

nanowires, the subsequent nanowire keeps both the easiest growth and the most stable state, and maintains a directed crystal lattice that is identical to the original one. The rocket-shaped nanowires form with a single crystal-like nature. When the flux of the source gases increases further to 40 sccm, the excess of TiSi will precipitate on the side-wall of TiSi nanowires. As shown in Figure 6d, some particles are deposited on the side-wall of TiSi rocket-shaped nanowires.

The formation progress of the TiSi rocket-shaped nanowires can be schematically shown in the diagram of Figure 8. The TiSi nanowires mainly originated from the quasi-liquid Ti−Si nanoislands[17] that formed on the Ti_5Si_3 film. We have found that the nanoislands formed are related to the reaction of excess Si with the Ti_5Si_3 phase in the film. As discussed above, the quantity of TiSi increases with an increase in the concentration of the source gases. The excess of TiSi will form a new nucleus. Finally, the new nanowires form due to the induction effect of the original TiSi nanowires.

Three kinds of TiSi nanowires have been successfully prepared. Moreover, a novel assembled structure composed of electrically conductive shrubbery TiSi nanowires and an electrically conductive Ti_5Si_3 thin layer underneath is also obtained, as shown in Figure 1d. The novel assembled structure can be used as a nanowire bottom electrode for the thin film devices because the fringing electric fields radiated from the nanowires' surfaces can be used effectively. Figure 9 shows the C (capacitance)-f (frequency) and L (loss)-f (frequency) curve of the BST thin film embedded with and without the nanowire-assembled bottom electrode. The capacitance per unit thickness of the BST with the nanowire electrode embedded in is about 28 pF, which is about 3 times higher than that of the BST deposited on ITO glass. The loss tangent is only about 0.04.

When the BST thin film is deposited on the assembled structure, the nanowires are embedded in the BST dielectric, so the fringing electric fields radiating from the nanowire surfaces are better confined within the thin film. Both the homogeneous fields and the fringing electric fields radiated between the nanowire surfaces and the top electrode can be used effectively. A higher intensity of effective electric field can be thus obtained. As a result, a higher capacitance is exhibited, as shown in Figure 9. Obviously, the new assembled capacitor has a high charge storage capability. That is to say, the assembled structure of electrically conductive nanowires growing on the electrically conductive thin film is acceptable for use as an assembled electrode for a high quality thin film capacitor.

4. Conclusions

The single crystalline orthorhombic TiSi nanowires were successfully prepared on Ti_5Si_3 layer by APCVD. TiSi nanowires grow along the direction perpendicular to (110) plane of the orthorhombic TiSi crystal. Nanowires with diameters of 15−40 nm and lengths of about 5 μm were obtained. When the flux of source gases of (SiH_4 + $TiCl_4$) was changed from 20 to 35 sccm, the excess TiSi forms a new nucleus on the tip of the nanowires. Due to the induction effect of the TiSi nanowires, the new nanowires form and encircle the central long nanowire. Rocket-shaped nanowires form. With the flux of source gases of (SiH_4 + $TiCl_4$) at a higher value (35 sccm), the TiSi nanowire bundles, which consist of several parallel nanowires, were also prepared with the same formation process. Moreover, a novel assembled structure composed of electrically conductive shrubbery TiSi nanowires and an electrically conductive Ti_5Si_3 thin layer underneath is obtained. As an application to a high storage capacitor, a BST dielectric thin film with the nanowire bottom electrode embedded in is successfully

prepared. Under the fringing electric fields radiated from the nanowires' surfaces, the capacitance of BST thin film is about 28 pF, which is approximately 3 times higher than that of BST deposited on ITO glass. Thus, this method creates a new way in which to fabricate thin film devices with high performances.

Acknowledgment. This work is financially supported by the National Natural Science Foundation of China (Grant No. 50672084) and the National Key Scientific and Technological Project (Grant No. 2008CB613302).

References

(1) Kuykendall, T.; Pauzauskie, P. J.; Zhang, Y. F.; Goldberger, J.; Sirbuly, D.; Denlinger, J.; Yang, P. D. *Nat. Mater.* **2004**, *3*, 524–528.
(2) Wagner, R. S.; Ellis, W. C. *Appl. Phys. Lett.* **1964**, *4*, 89–90.
(3) Persson, A.; Larsson, M. W.; Stenstrom, S.; Ohlsson, B. J.; Samuelson, L.; Wallenberg, L. R. *Nat. Mater.* **2004**, *3*, 677–681.
(4) Kamins, T. I.; Williams, R. S.; Basile, D. P.; Hesjedal, T.; Harris, J. S. *J. Appl. Phys.* **2001**, *89*, 1008–1016.
(5) Snow, E. S.; Perkins, F. K.; Houser, E. J.; Badescu, S. C.; Reinecke, T. L. *Science* **2005**, *307*, 1942–1945.
(6) Huang, J.; Du, P.; hong, L.; Dong, Y.; Hong, M. *Adv. Mater.* **2007**, *19*, 437–440.
(7) Homes, C. C.; Vogt, T.; Shapiro, S. M.; Wakimoto, S.; Ramirez, A. P. *Science* **2001**, *293*, 673–675.
(8) Zhou, X. L.; Du, P. Y. *Acta Phys. Sin.* **2005**, *54*, 1809–1813.
(9) Pecharroman, C.; Betegón, F. E.; Bartolome, J. F.; Esteban, S. L.; Moya, J. S. *Adv. Mater.* **2001**, *13*, 1541–1544.
(10) Lee, J.; Reif, R. *J. Electron. Mater.* **1991**, *20*, 331–337.
(11) He, Z.; Smith, D. J.; Bennett, P. A. *Phys. Rev. Lett.* **2004**, *93*, R256102.
(12) Chen, Y.; Ohlberg, D. A. A.; Williams, R. S. *Mater. Sci. Eng., B* **2001**, *87*, 222–226.
(13) Li, C. P.; Wang, N.; Wong, S. P.; Lee, C. S.; Lee, S. T. *Adv. Mater.* **2002**, *14*, 218–221.
(14) Luo, J.; Zhang, L.; Zhu, J. *Adv. Mater.* **2003**, *15*, 579–581.
(15) Xiang, B.; Wang, Q. X.; Wang, Z.; Zhang, X. Z.; Liu, L. Q.; Xu, J.; Yu, D. P. *Appl. Phys. Lett.* **2005**, *86*, 243103.
(16) Ragana, R.; Chen, Y.; Ohlberg, D. A. A.; Medeiros-Ribeiro, G.; Williams, R. S. *J. Cryst. Growth* **2003**, *251*, 657–661.
(17) Du, J.; Du, P.; Hao, P.; Huang, Y.; Ren, Z.; Weng, W.; Han, G.; Zhao, G. *Nanotechnology* **2007**, *18*, 345605.
(18) Du, J.; Du, P.; Xu, M.; Hao, P.; Huang, Y.; Han, G.; Song, C.; Weng, W.; Wang, J.; Shen, G. *J. Appl. Phys.* **2007**, *101*, 033539.
(19) Cramer, N.; Mahmud, A.; Kalkul, T. S. *Appl. Phys. Lett.* **2005**, *87*, 032903.
(20) Reynolds, G. J.; Cooper, C. B.; Gaczi, P. J. *J. Appl. Phys.* **1989**, *65*, 3212–3218.
(21) Du, J.; Du, P.; Hao, P.; Huang, Y.; Ren, Z.; Weng, W.; Han, G.; Zhao, G. *J. Phys. Chem. C* **2007**, *111*, 10814–10817.

CG7008545